A head-to-head comparison of ^{18}F-FDG PET/CT and ^{18}F-FDG PET/MR in patients with nasopharyngeal carcinoma under different disease settings

Mengxia Zhang[1,2,3,4#] **MD, PhD,**
Lifang Pang[1,2,3,4#] **MD, PhD,**
Haojun Yu[1,2,3,4]
Hongcheng Shi[1,2,3,4] **MD, PhD**

#Mengxia Zhang and Lifang Pang contributed equally to this work.

1. Department of Nuclear Medicine, Zhongshan Hospital, Fudan University, 180 Fenglin Rd., Shanghai, China
2. Institute of Nuclear Medicine, Fudan University, Shanghai, China
3. Shanghai Institute of Medical Imaging, Shanghai, China
4. Cancer Prevention and Treatment Center, Zhongshan Hospital, Fudan University, Shanghai 200032, China

Keywords: Nasopharyngeal carcinoma - PET/CT - PET/MR - Diagnostic performance - Head-to-head comparison

Corresponding author:
Hongcheng Shi MD, PhD, Department of Nuclear Medicine, Zhongshan Hospital, Fudan University, 180 Fenglin Rd, Shanghai, 200032, China.
Shi.hongcheng@zs-hospital.sh.cn

Received:
18 May 2024
Accepted revised:
15 July 2024

Abstract

Objective: Positron emission tomography/computed tomography (PET/CT) and magnetic resonance imaging (MRI) are complementary in staging of nasopharyngeal carcinoma (NPC). The combination of MRI and functional imaging from PET in PET/MR is promising in NPC management. Diagnostic performance of PET/CT and PET/MR was compared in 46 patients with histologically confirmed NPC under different disease scenarios, including primary non-metastatic cases, primary metastatic cases, recurrence and/or metastasis after treatment, and post-treatment follow-up cases. **Subjects and Methods:** Forty-six patients underwent both PET/CT and PET/MR in the same day. Primary tumor extension into risk-stratified anatomic structures, retropharyngeal and cervical lymph node metastasis, distant metastasis and post-treatment follow-up results, were compared. **Results:** For high-risk structures, PET/MR detected two more sides of tensor/levator veli palatine muscle involvement, one more case of clivus involvement, and ruled out 12 false-positive sides of prevertebral muscle involvement by PET/CT. For medium-risk structures, PET/MR detected four more sides of medial pterygoid muscle involvement. For low-risk structures, abnormal signal on massa lateralis atlantis was detected by PET/MR. Positron emission tomography/MR detected 14 more positive retropharyngeal lymph nodes and more liver micrometastases than PET/CT. Overall, PET/MR changed two patients' T staging. **Conclusions:** Positron emission tomography/MR outperforms PET/CT in delineating muscle, skull-base bone, and nodal involvement, and identifying liver micrometastases, may serve as a single-step staging modality for NPC.

Hell J Nucl Med 2024; 27(2): 93-104 *Epub ahead of print: 6 August 2024* *Published online: 28 August 2024*

Introduction

Nasopharyngeal carcinoma (NPC) is the most common type of head and neck cancer in Southeast Asia, especially in South China [1]. Radiotherapy is the mainstay treatment for non-metastatic NPC, as it is high sensitive to radiation [1]. However, due to the complex anatomic structures surrounding the nasopharynx, delineating the target of NPC can be challenging. Liang et al. (2009) investigated the local extension patterns of NPC and classified the anatomic sites around the nasopharynx into three risk groups based on the incidence rates of tumor invasion: high risk (≥35%, including parapharyngeal space, levator/tensor veli palatine muscle, clivus, basis of sphenoid bone, nasal cavity, pterygoid process, medial pterygoid plate, foramen lacerum, etc.), medium risk (≥ 5%-35%, including medial pterygoid muscle, sphenoidal sinus, pterygopalatine fossa, foramen ovale, the great wing of sphenoid bone, etc.), and low risk (<5%, including cervical vertebrae, temporal lobe, orbital apex, maxillary sinus, meninges, etc.) [2]. Accurate identification of tumor extension into these risk-stratified structures and staging are crucial for treatment selection, particularly in terms of delineation and subsequent radiotherapy planning.

National comprehensive cancer network (NCCN) guidelines recommend magnetic resonance imaging (MRI) of the head and neck along with fluorine-18 fluorodeoxyglucose (^{18}F-FDG) positron emission tomography and computed tomography (PET/CT) imaging for diagnosis and staging of NPC. While positron emission tomography/computed tomography (PET/CT) is particularly helpful in identifying nodal and distant metastasis [3], its sensitivity in detecting primary tumor extension is limited due to the inadequate soft tissue resolution of CT [4, 5]. Simultaneous positron emission tomography and magnetic resonance (PET/MR) imaging, offers multi-parametric MRI and PET images that provide improved soft tissue contrast and additional functional information, which may allow for

better staging of NPC.

Several studies reported the use of PET/MR in the diagnosis and staging of NPC. A prospective study involving 113 patients with newly diagnosed NPC found that PET/MR was more accurate than the combination of head and neck MRI and PET/CT [6]. Cao et al. (2021) defined the loco-regional extension pattern of NPC by PET/MR in 331 non-metastatic NPC patients, demonstrating that the spread of the primary tumor and regional lymph node follows an orderly pattern, the skip metastasis of the lymph node was uncommon [7]. Cheng et al. (2020) performed PET/CT and PET/MR on 35 patients with NPC and showed that PET/MR provided better image quality, lesion conspicuity, and diagnostic confidence for NPC than PET/CT [8]. Another study based on 60 NPC cases reported that the overall accuracy of PET/MR for the staging of recurrent or metastatic NPC was 88.3%, indicating that it has the potential to be a single-step modality for staging [9].

However, comparative studies of PET/CT and PET/MR based on the reported NPC invasion map and under different disease scenarios are limited. In this study, a head-to-head comparison was conducted to determine if simultaneous PET/MR is superior to PET/CT for evaluation of primary tumor extension, nodal involvement, distant metastasis, and post-treatment follow-up status in NPC patients in a high-incidence area.

Subjects and Methods

Patients

From May 2018 to March 2022, 46 patients with NPC were included in the study. Inclusion criteria were: i) biopsy-proven NPC, ii) no contraindications to MRI, iii) serum glucose level <10mmol/L before PET/CT scan, and iv) the ability to provide written informed consent. Patients with a history of previous head and neck malignancies, or concomitant cancers in different anatomical locations were excluded. All patients were staged according to the 8th edition of the American Joint Committee on Cancer (AJCC)/Union for International Cancer Control (UICC) staging system.

The participants signed an informed consent form after completing routine PET/CT and then undergoing PET/MR. Medical records and imaging studies were reviewed retrospectively and additional informed consent was waived. The study protocol was approved by the Institutional Review Board of our Hospital (IRB no. B2023-269).

^{18}F-FDG PET/CT and ^{18}F-FDG PET/MR

All patients were required to fast for at least 6 hours to maintain serum glucose levels below 10mmol/L before the injection of ^{18}F-FDG (approximately 3.6MBq/kg). Positron emission tomography/CT imaging was acquired approximately 60min after the injection using mostly uMI550/780/uEXPLORER scanner (United Imaging Healthcare) (Table 1). Four cases were scanned using the Discovery VCT 64 scanner (GE Healthcare) (Table 2). The parameters used for the CT scan were: Current 120-270mAs; Voltage 120-140kV; Pitch 0.516-0.625. Various CT windows (soft-tissue, lung, liver, bone window, etc) were used to optimize visualization of specific tissues or abnormalities. Positron emission tomography images were acquired for 2-3 min per bed position in 3D mode. Computed tomography scans were reconstructed using a matrix of 512×512. Positron emission tomography scans were reconstructed with a matrix of 128×128 using the ordered subset expectation maximization (OSEM) algorithm and CT-based attenuation correction.

After the PET/CT acquisition, a whole-body PET/MR scan was performed using the uPMR790 HD TOF PET/MR containing a 3.0-Tesla MR imager and an integrated PET detector (United Imaging Healthcare). Further details regarding PET/MR scan have been described in previous studies [10, 11]. Briefly, PET images and MRI sequences, including T1 weighted images (T1WI), T2 weighted images (T2WI) with and without fat saturation (T2-fs), and diffusion-weighted images (DWI), were acquired at axial, sagittal, and coronal plane positions. Whole-body PET scans were performed in four bed positions with three minutes per bed position, from the head to the upper thigh. Positron emission tomography imaging was done regionally for 15 minutes, and MRI scans of the head and neck area were obtained. The PET images were reconstructed using a standard process provided by the vendor, which included TOF-OSEM with 20 subsets and 3 iterations, an image matrix of 150×150, a voxel size of 2.4×2.4×2.85mm^3, and a 3mm post-Gaussian filter.

Image interpretation and diagnostic criteria

The image interpretation was performed independently by two nuclear medicine physicians. They were blind to the clinical information and diagnostics. Any discordant cases were discussed to reach a consensus.

T staging assessment

The reference standard for T staging of NPC included nasopharyngoscopy to detect mucosal extension and MRI to identify submucosal extension [6]. Detailed diagnostic criteria for anatomic structure invasion surrounding the nasopharynx were reported in a previous study [7].

In the case of pathological diagnosis, any submucosal abnormalities observed on MRI were considered to be the result of tumor infiltration since current clinical practice is to encompass all abnormal areas in the irradiation field, thereby ensuring the inclusion of all regions with potential microscopic disease [12].

On PET/CT images, lesions with ^{18}F-FDG uptake that exceeded those of surrounding tissues were identified as having tumor infiltration. The maximum of standardized uptake value (SUVmax) of the region of interest (ROI) was measured on PET image, and corresponding CT image helped identify the morphology and localization of the lesions.

N staging assessment

The 2013 updated consensus guideline of the neck node levels was used to determine cervical lymph node (CLN) levels [3]. On MR or CT image, metastatic CLN was defined based on morphological criteria, which included: i) the presence of necrosis or extracapsular spread, ii) the shortest axial diameter was ≥5mm in the retropharyngeal region or ≥10mm in other

Table 1. *The distribution of PET/CT scanner used in the cohort.*

Scanner	uMI-550	uMI-780	uEXPLORER	GE Discovery VCT 64
No. of patients	11	23	11	4

Table 2. *Specific information of 4 patients using GE Discovery VCT 64.*

			PET/CT	PET/MR
#1	Primary non-metastatic	T	Left pharyngeal recess, left tensor/Levator veli palatine muscle, left medial pterygoid muscle, bilateral prevertebral muscle, clivus, left foramen lacerum, left foramen ovale, basis of sphenoid bone	Left pharyngeal recess, left tensor/Levator veli palatine muscle, left medial pterygoid muscle, bilateral prevertebral muscle, clivus, left foramen lacerum, left foramen ovale, basis of sphenoid bone
		N	Right IIB, left IIA, IIB, VA	Right IIB, left IIA, IIB, VA
		M	/	/
#2	Primary metastatic	T	Right pharyngeal recess	Right pharyngeal recess
		N	Right IIB	Right IIB
		M	Liver metastasis (5 lesions)	Liver metastasis (>10 lesions)
#3	Post-treatment metastatic	T	/	/
		N	Left IB, IV, right IB	Left IB, IV, right IB
		M	Right parotid gland, left occipital posterior region, bone (multiple)	Right parotid gland, left occipital posterior region, bone (multiple)
#4	Post-treatment follow-up	T	/	/
		N	/	/
		M	/	/

T=primary tumor, N=locoregional lymph node metastasis, M=distant metastasis

regions of the neck, iii) a cluster of two or more lymph nodes of borderline size [14]. On PET images, metastatic CLN was defined as: i) ^{18}F-FDG uptake exceeded the surrounding normal tissue, ii) asymmetric metabolic activity greater than that of normal lymph nodes at the same level in the contralateral neck [15].

M staging assessment

The presence of distant metastasis was determined based on the ^{18}F-FDG uptake and the lesion's morphology displayed on MRI or CT, as mentioned above.

Statistical analysis

Statistical analysis was conducted using SPSS Statistics 26.0. Data were tested for normality. Mean±SD and median (range) were used to present normal-distributed variables and skewed variables, respectively.

Results

Clinical characteristics

The patient characteristics are shown in Table 3. A total of 37 male and 9 female patients with pathologically confirmed NPC, aged from 28 to 74 years old (median, 54.5 years), were enrolled. Among them, 25 had newly diagnosed non-metastatic NPC, while four were recurrent NPC. Two and eight patients developed distant metastasis at the initial diagnosis and after curative treatment, respectively. Two patients developed simultaneous primary tumor recurrence and distant metastasis. The remaining five patients had sequela or negative results after curative treatment. The median blood glucose level was 5.6mmol/L. The radiotracer average dose was 3.6±0.8MBq/kg. The mean delay of PET/MR was 1.3 hours (range: 0.3-3 hours).

Comparison of PET/CT and PET/MR in evaluating primary tumor invasion (T staging) into risk-stratified anatomic structures

The 36 analyzable cases including 25 patients with primary non-metastatic NPC, four with recurrent NPC, two with primary metastatic NPC, three with metastasis after treatment, and two with simultaneous recurrence and metastasis after treatment. As shown in Table 4, PET/MR was superior to PET/CT in identifying tensor/levator veli palatine muscle involvement (Figure 1a) and clivus invasion (Figure 2a) in the high-risk structures. Positron emission tomography/MR ruled out false-positive results in 12 sides of prevertebral muscle on PET/CT (Figure 1b). Additionally, PET/MR detected three more sides of medial pterygoid muscle involvement (Figure 1c) in the medium-risk structures, and one left massa lateralis atlantis involvement (Figure 2b, Figure 3) in the low-risk structures.

Comparison of PET/CT and PET/MR in the evaluation of regional lymph node involvement (N staging)

Positron emission tomography/MR identified 49 positive retropharyngeal lymph nodes (RLN) in 30 patients, while PET/CT identified 35 positive RLN in 25 patients (Table 5, Figure 4a). Positron emission tomography/MR and PET/CT were identical in identifying the involved regions of CLN, with a total of 111 regions detected. Level IIb (40, 36.0%) was the most frequently involved level, followed by level IIa (36, 32.4%), level III (16, 13.8%), level Va (9, 8.1%), level IV (7, 6.3%) and level Ib (3, 2.7%). No nodal metastasis was observed in level Ia and Vb, and skip metastasis was not found (Table 5). Additionally, PET/MR clearly outlined the borders of positive CLNs (Figure 4b).

Table 3. *Clinical information and patient characteristics (n=46).*

Characteristics	Patients (%)
Disease state	
Primary non-metastatic (untreated)	25 (54.4%)
Primary metastatic (untreated)	2 (4.3%)
Recurrence after treatment	4 (8.7%)
Metastasis after treatment	8 (17.4)
Simultaneous recurrence and metastasis after treatment	2 (4.3%)
Follow-up (developed sequela or normal)	5 (10.9%)
Sex	
Male	37 (80.4%)
Female	9 (19.6%)
Age, Median (range), years	54.5 (28-74)
Height, (Mean±SD), cm	167.7±6.6
Body weight, (Mean±SD), kg	65.7±10.6
Dose, Mbq/kg (Mean±SD)	3.6±0.8
Blood glucose, Median (range), mmol/L	5.6 (4.4-9.9)
PET/MR delay, Mean (range), hours	1.3 (0.3, 3.0)

SD=standard deviation

Table 4. *Incidence of tumor invasion into risk-stratified anatomic sites surrounding the nasopharynx for analyzable cases*.*

Anatomic sites	No. of cases or sides		Anatomic sites	No. of cases or sides		Anatomic sites	No. of cases or sides	
	PET/CT	PET/MR		PET/CT	PET/MR		PET/CT	PET/MR
High risk			Medium risk			Low risk		
Tensor/Levator veli palatine muscle#	21	23	Medial pterygoid muscle#	11	15	Cervical vertebrae※	0	1
Prevertebral muscle#	40	28	Sphenoidal sinus	4	4	Temporal lobe#	1	1
Clivus	14	15	Pterygopalatine fossa#	3	3	Orbital apex#	1	1
Basis of sphenoid bone	14	14	Cavernous sinus#	4	4	Maxillary sinus#	1	1
Nasal cavity	4	4	Foramen ovale#	5	5	Pituitary fossa	1	1
Pterygoid process#	7	7	Hypoglossal canal#	1	1	Meninges	0	0
Medial pterygoid plate#	12	12	Lateral pterygoid muscle#	1	1	Superior orbital fissure	0	0
Foramen lacerum#	8	8	Foramen rotundum#	1	1	Inferior orbital fissure	0	0
Vomer bone	7	7	Ethmoid sinus	1	1	Infratemporal fossa	0	0
Petrous apex#	3	3	Great wing of sphenoid bone	0	0	Cerebral cistern	0	0
Occipital bone	3	3	Jugular foramen	0	0	Hypopharynx	0	0
Lateral pterygoid plate#	1	1	Oropharynx	0	0	Frontal sinus	0	0

**Thirty six patients who have primary nasopharyngeal lesions: primary non-metastatic (n=25), primary metastatic (n=2), recurrence after treatment (n=4), metastasis after treatment (n=3), Simultaneous recurrence and metastasis after treatment (n=2). Sides and cases were used for symmetrical structures and nonsymmetrical structures, respectively. #For symmetrical structures, bilateral structural involvement were calculated as two. ※left massa lateralis atlantis.*

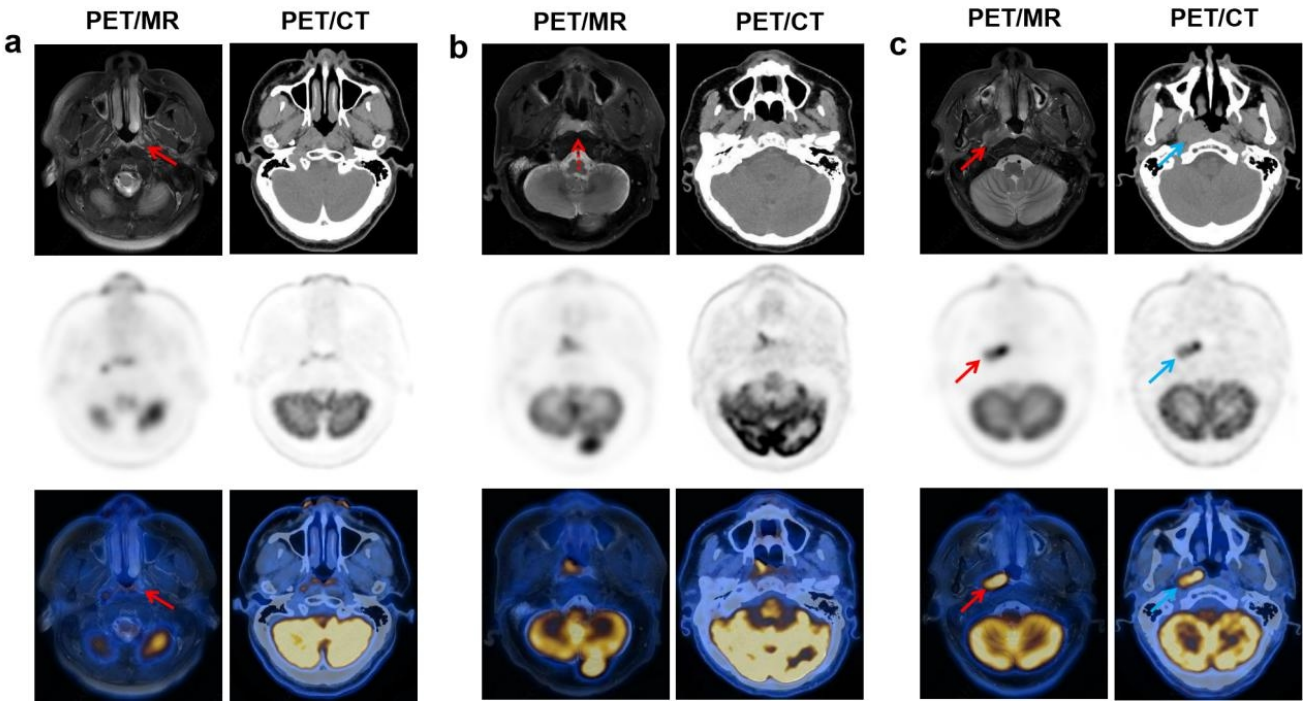

Figure 1. Detection of muscle extension. Each panel: top (MRI T2-fs or CT), middle (PET), and bottom (fused image). (a) The left tensor/levator veli palatine muscle was involved on PET/MR (red arrow), while was misjudged as normal on PET/CT (right column); (b)PET/MR was rated as negative for prevertebral muscle involvement as the mucosa line is intact (red dashed arrow), while was misjudged as positive on PET/CT (right column). (c) Medial pterygoid muscle was involved on PET/MR (red arrow), while cannot be distinguished on PET/CT and was rated as negative (blue arrow).

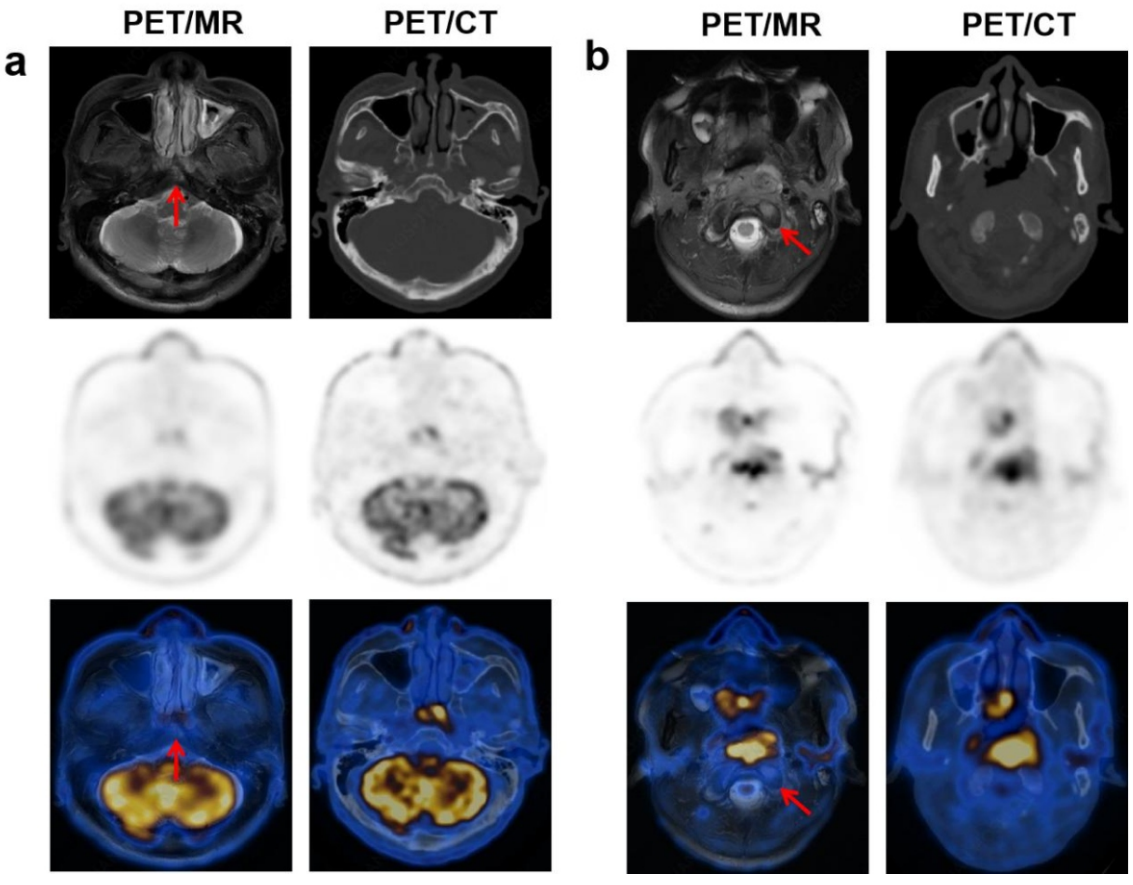

Figure 2. Detection of skull base bone involvement. Each panel: top (MRI or CT), middle (PET), and bottom (fused image). PET/CT was unable to determine the clivus (a, red arrow) and left massa lateralis atlantis (b, red arrow) involvement, while PET/MR revealed their signal abnormality with hyperintense areas on T2-fs.

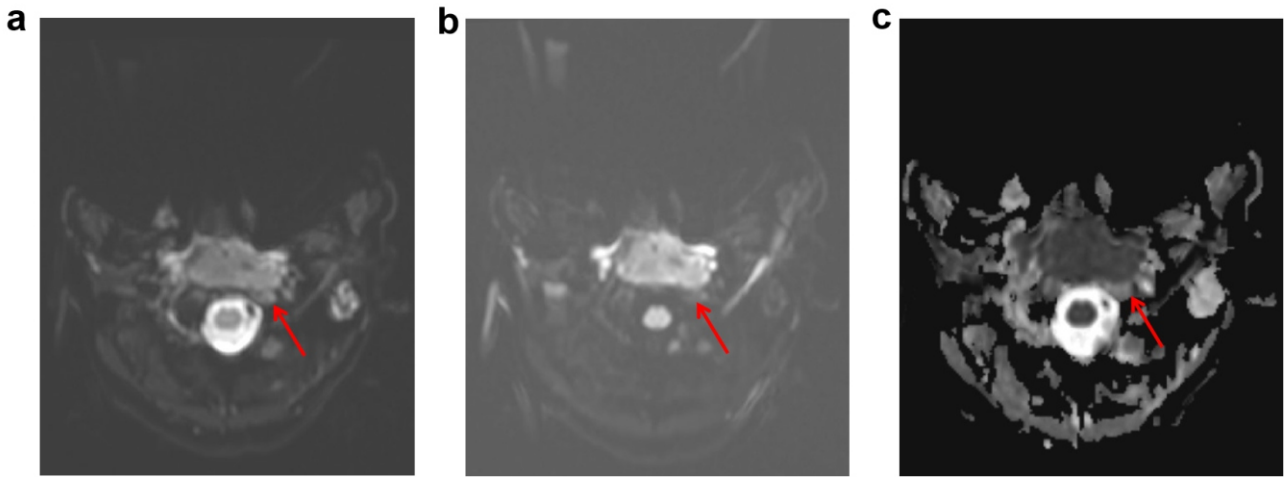

Figure 3. The b0 (a) and b1000 (b) images demonstrating high signal intensity and the corresponding apparent diffusion coefficient (ADC) image (c) showing low signal intensity in the lest massa lateralis atlantis lesion.

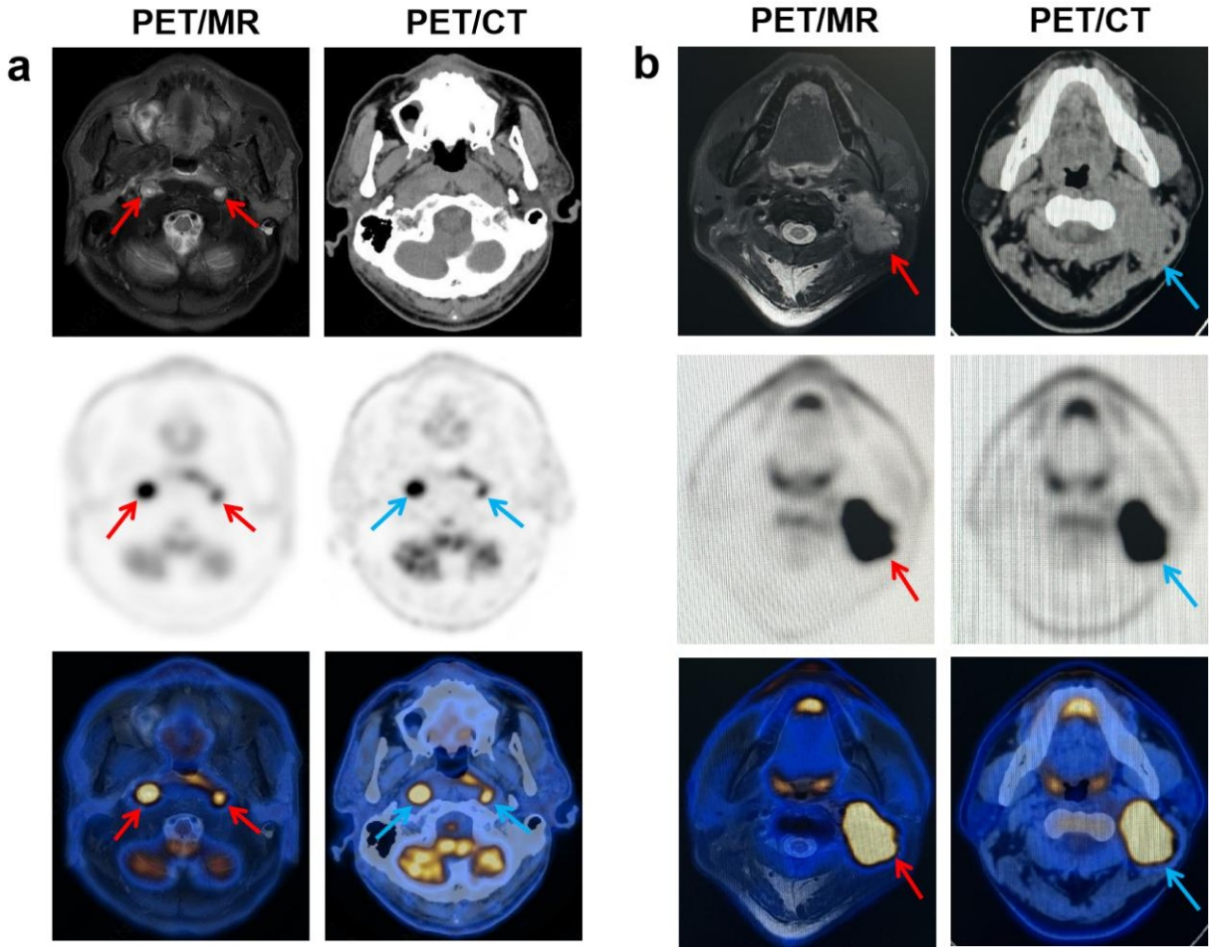

Figure 4. Detection of lymph node metastasis. Each panel: top (MRI or CT), middle (PET), and bottom (fused image). (a) PET/MR can separate bilateral sides of retropharyngeal lymph nodes (RLN) from the primary tumor (red arrow), while the RLNs were merged with the primary tumor on PET/CT (blue arrow); (b) PET/MR clearly shows the border of positive cervical lymph nodes (CLN) and their correlation with adjacent muscles (red arrow), while CLN were merged with adjacent muscles in PET/CT (blue arrow).

Comparison of PET/CT and PET/MR in the evaluation of distant metastasis (M staging)

Two patients had primary metastatic NPC (de novo metastasis) and 10 developed distant metastases after curative treatment were analyzed. Specifically, PET/MR identified more liver micro-metastases compared to PET/CT in three cases. These liver micro-metastases were either indistinct or undetected on PET/CT (one scanned by GE, one by uMI-550, the other one by uMI-780) (Figure 5a, Figure 6). In four cases, PET/MR detected the same number of relatively certain lung and bone metastases as PET/CT (Figure 5b-c, Table 6), while PET/MR fails to display small (≤5mm) and ground-grass lung nodules.

Table 5. *Incidence of nodal spread for analyzable cases*.*

	PET/CT	PET/MR
RLN		
Total number	35	49
Left side	15	21
Right side	20	28
CLN		
Total regions	111	111
L-Ia	0	0
R-Ia	0	0
L-Ib	0	0
R-Ib	3	3
L-IIa	15	15
R-IIa	21	21
L-IIb	18	18
R-IIb	22	22
L-III	6	6
R-III	10	10
L-IV	3	3
R-IV	4	4
L-Va	4	4
R-Va	5	5
L-Vb	0	0
R-Vb	0	0

**patients who have RLN and/or CLN metastasis. RLN=retropharyngeal lymph node; CLN=cervical lymph node; L=left; R=right*

Changes in the overall staging

One patient was down-staged to Stage I by PET/MR due to a misjudgment of prevertebral muscle involvement on PET/CT. Another patient with recurrent NPC was up-staged to Stage II due to the detection of medial pterygoid muscle involvement on PET/MR.

Comparison of PET/CT and PET/MR in other disease settings

For patients who had received radical treatment and scanned for follow-up, PET/MR clearly display the range of temporal lobe necrosis and the internal morphological characteristics in one case (Figure 7).

Discussion

This study showed that integrated PET/MR had better diagnostic performance than PET/CT for assessing local tumor invasion and RLN metastasis. Positron emission tomography/MR was identical to PET/CT in determining the involved CLN regions. Additionally, PET/MR detected more liver micro-metastases than PET/CT in the limited cases. Furthermore, PET/MR provided a better anatomic reference that facilitated outlining the border of lesions, which was crucial for target delineation of NPC for radiotherapy.

Typically, the weakness of PET/CT lies in the inferior soft tissue resolution compared to MRI [16-18]. Magnetic resonance imaging has the advantage of assessing parapharyngeal spaces, intracranial invasion, and retropharyngeal and supraclavicular lymph nodes in NPC [19]. In this cohort, the superiority of integrated PET/MR lies in recognizing muscle involvement and skull base invasion. Clear soft tissue resolution of PET/MR is apparent. Controversy exists in the identification of bony involvement. Karsten et al. (2014) conducted a prospective study involving 67 patients with solid tumors who underwent both PET/CT and PET/MR scans; Similarly, PET/MR offers superior lesion conspicuity compared to PET/ CT when evaluating bone metastases [20]. According to NCCN guideline, MRI is generally preferred over CT to evaluate tumors that encroach on the skull base. Computed tomography, conversely, is a complementary to MRI for evaluation of bony erosion or cartilage invasion [3]. We observed bony involvement in two patients with untreated primary NPC, thus ruling out osteoradionecrosis. As discussed in Lofgren's article (2017) [21], the pathology of bone metastasis was hard to be obtained due to the impracticality of obtaining multiple biopsy specimens from one patient, particularly for skull base bone involvement. It can be argued that not all abnormalities detected by MRI can be solely attributed to tumor infiltration. Nevertheless, the current standard practice is to be cautious and include all areas of abnormality within the radiation field in order to eradicate microscopic disease [12]. Nasopharyngeal cancers are generally not resected; therefore, primary tumor extension is mainly evaluated through nasopharyngeal biopsy and MRI. A study indicated that the sensitivity of PET/MR (99.5%) was higher than that of head and neck MRI (94.2 %) and was even more accurate than the combination of MRI and PET/CT in the staging of NPC [6].

Nasopharyngeal carcinoma has a tendency to metastasize to cervical lymph node, and RLN is considered as the sentinel node [1]. In our cohort, PET/MR detected more suspicious metastatic RLN than PET/CT. The discrepancy was attributed to the merging of some RLNs with primary tumors in PET/CT. Conversely, MRI, especially T2-fs, accurately delineates the margins of lymph nodes, and is sensitive in detecting necrotic or cystic lymph nodes. The rates of lymph node

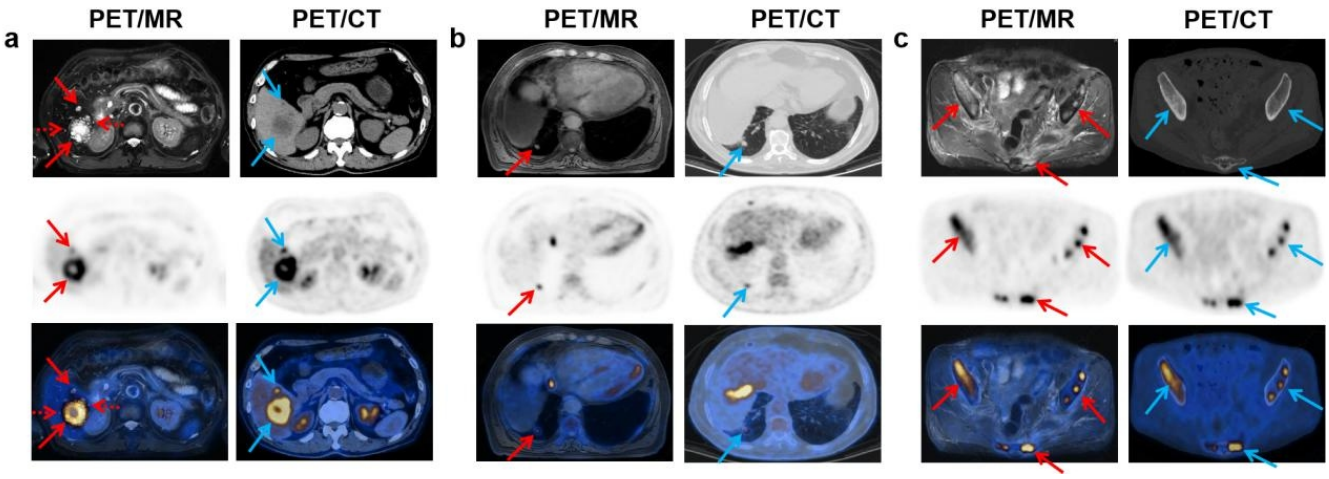

Figure 5. Detection of distant metastasis. (a) Liver metastasis detected on both PET/MR (red arrow) and PET/CT (blue arrow). Positron emission tomography/MR shows clear boundaries and internal morphology and detects more tiny lesions (red dashed arrow); (b) PET/MR (red arrow) and PET/CT (blue arrow) both displayed a lung metastatic lesion; (c) PET/MR (red arrow) and PET/CT (blue arrow) both showed metastases on bilateral iliac and sacral bones.

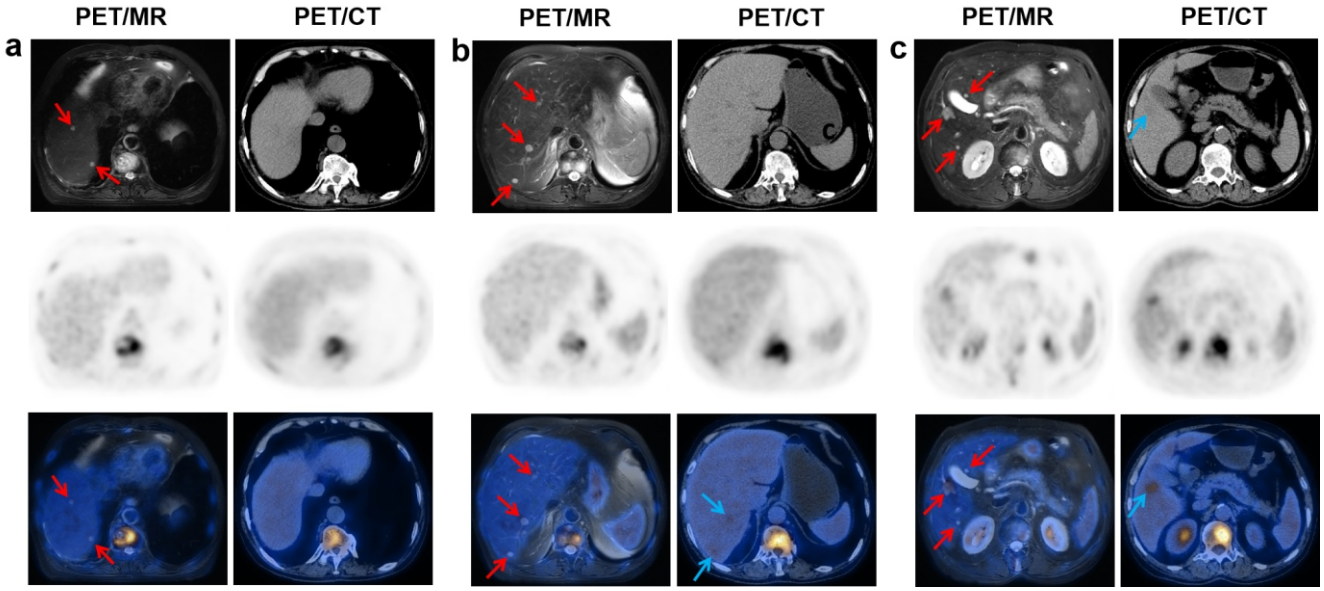

Figure 6. Comparison of a patient with liver metastasis scanned with GE Discovery VCT 64 scanner for PET/CT (a-c, right row) and PET/MR (a-c, left row). Positron emission tomography/MR detected more liver metastases compared to PET/CT.

metastasis from the upper neck to the lower neck decreased orderly, and skip metastasis was not found, which was consistent with the findings from previous studies [2, 7, 22]. Positron emission tomography/MR and PET/CT were identical in determining the involved cervical levels. However, PET/MR still provided clearer outlines of lesions, which may limit or accurately match the irradiation field, thus reducing radiotherapy-induced sequelae.

It should be noted that patients in our cohort did not maintain ultrasound-guided fine needle puncture (FNA) for CLN. According to the Chinese Society of Clinical Oncology (CSCO) clinical guidelines, the recommend level of FNA for regional lymph node is III (low-level) [23]. National comprehensive cancer network guideline recommends a biopsy of the primary site or FNA of the neck (alternatively) for the clinical workup of NPC. Lymph node metastasis was mainly determined non-invasively based on imaging modalities [3]. Positron emission tomography/CT can assess T, N, and M stages of NPC simultaneously and false-negative micrometastatic neck nodes could be treated with prophylactic whole-neck irradiation [5].

For overall staging, one patient was down-staged to stage I and one was up-staged to stage II on PET/MR. This may lead to management changes, patients with stage I NPC typically receive radiotherapy alone, while stage II NPC may require additional concurrent chemotherapy alone with radiotherapy [1]. Furthermore, the crucial aspect is the impact on the external beam radiation therapy gross tumor volume deline-

Table 6. *The detail information of lung and/or bone metastases in this cohort.*

	Mets site	PET/CT	PET/MR
#1	bone	Skull base bone, spine, pelvis, bilateral ribs, sternum, bilateral scapula, and bilateral upper femur	equivalent to PET/CT
#2	bone	Skull base bone, left scapula, multiple vertebral bodies of the spine, and upper left femur	equivalent to PET/CT
#3	lung	Several small nodules in both lungs, some with increased glucose metabolism; Several ground glass nodules in the right lung; Mediastinum, bilateral hilar, bilateral internal mammary, and superior phrenic enlarged lymph nodes; Local nodular thickening of bilateral pleura; Minor pleural effusion on both sides	The display of nodules smaller than 5mm and ground-glass nodules can be more challenging with PET/MR compared to PET/CT, while the display of other lesions is equivalent to that of PET/CT
	bone	Skull base bone, spine, sternum, bilateral scapula, right clavicle, bilateral multiple ribs, pelvic bone, right humerus, bilateral femur	equivalent to PET/CT
#4	lung	Right upper lobe posterior segment (2 lesions), lower lobe posterior basal segment, and left upper lobe apical posterior segment	equivalent to PET/CT

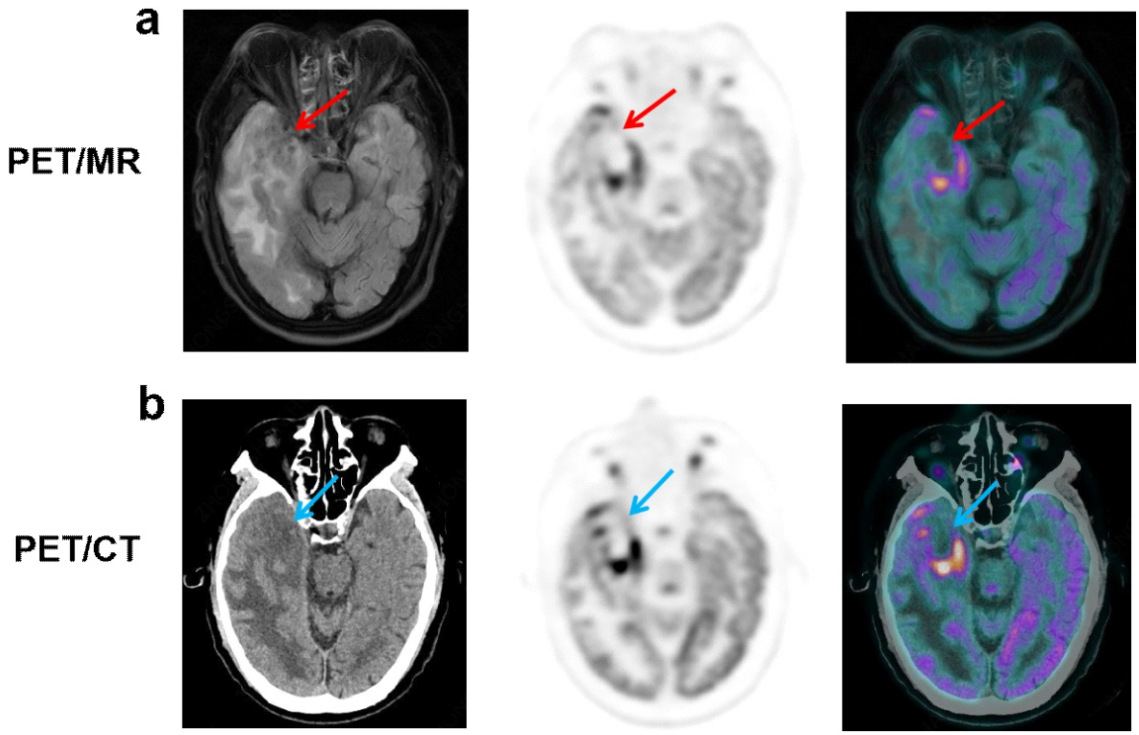

Figure 7. Detection of radiotherapy complications between PET/CT and PET/MR. Each panel: left (MRI or CT), middle (PET), and right (fused image). Right temporal lobe necrosis was detected both on PET/MR (a, red arrow) and PET/CT (b, blue arrow). PET/MR could provide more internal morphological characteristics.

ation. By accurately defining tumor margin with PET/MR, the radiation field can be tailored to reduce radiation volume.

Despite recent advancement in treatment modalities, locoregional recurrence still occurs in 10%-20% of cases in early-stage disease and up to 30% of cases in locally advanced disease after definitive treatment [24, 25]. In this cohort, only six patients with recurrent NPC were analyzed, and PET/MR detected left medial pterygoid muscle involvement in one patient and ruled out a false-positive prevertebral muscle involvement in another. Accurate detection and early diagnosis of recurrent and/or residual tumor may improve patient's prognosis since localized disease is potentially salvageable [25]. Positron emission tomography/CT is still challenging for early detection of recurrent NPC due to treatment-induced tissue alterations and inflammatory conditions that can mimic disease activation [26]. Queiroz et al. (2014) compared PET/MR with PET/CT in 87 patients with suspected recurrence of head and neck cancer and suggested that PET/MR may be better at specifying possible tumor recurrence with obscure ^{18}F-FDG uptake than PET/CT [27]. Positron emission tomography/MR has been recommended as an alternative modality to PET/CT in post-chemoradiotherapy evaluation [28].

Apart from tumor recurrence, distant metastasis is the primary cause of death in NPC. Zhou et al. (2021) reported that the diagnostic performance of PET/MR is superior to that of PET/CT in detecting liver metastasis [29]. Similarly, PET/MR resulted in more liver lesions detected in our study. The improved diagnostic accuracy may have an impact on treatment decisions. A typical example is resectable colorectal cancer with liver metastasis, where the number of liver lesions determines the possibility of surgical resection and the need for neoadjuvant therapy [29]. However, one patient with liver metastasis was scanned by GE Discovery VCT 64 that is showing its age, and may not offer the same capabilities for PET imaging. The finding that PET/MR detects more liver metastases is partially due to a generation of improvement in device technology. Therefore, the results still need further confirmation.

Limitations

Firstly, due to the single injection and double examination pattern, the improved lesion detection ability of PET/MR may partly attribute to the delayed PET acquisition. Secondly, the study cohort was relatively small, especially under certain disease settings such as recurrent or metastatic cases. Thirdly, pathological confirmation of cervical lymph nodes and metastatic lesions were not performed. Last but not the least, the PET/MR scans were conducted using a restricted research protocol. A comprehensive clinical protocol would also include T1W spin echo sequence with gadolinium contrast enhancement. However, in a previous study, Lennart Flygare et al. (2023) [30] suggested that T2W fat-saturated images possibly be more sensitive for nodes and can result in more accurate tumor delineation. Pyatigorskaya et al. (2020) [31] also found that gadolinium contrast did not provide additional benefit for delineating tumors in head and neck MRI.

In conclusion, PET/MR provides valuable information on primary tumor extension, nodal involvement, distant metastasis, and post-treatment status, which may serve as a single-step staging modality for NPC. Further studies are needed to determine which patients would benefit most from PET/MR, and to investigate the survival benefit of PET/MR-guided dose painting and involved neck level radiotherapy for NPC patients.

Grant support

This study was supported by grants from the National Key Research and Development Program of China (2022YFC2406902), the Shanghai Municipal Key Clinical Specialty Project (SHSLCZDZK03401), Shanghai Science and Technology Project (19DZ1930700), the Shanghai Science and Technology Committee Program (20DZ2201800), the Three-year Action Plan of Clinical Skills and Innovation of Shanghai Hospital Development Center (SHDC2020CR3079B).

Bibliography

1. Chen YP, Chan ATC, Le QT et al. Nasopharyngeal carcinoma. *Lancet* 2019; 394(10192): 64-80.
2. Liang SB, Sun Y, Liu LZ et al. Extension of local disease in nasopharyngeal carcinoma detected by magnetic resonance imaging: improvement of clinical target volume delineation. *Int J Radiat Oncol Biol Phys* 2009; 75(3): 742-50.
3. Pfister DG, Spencer S, Adelstein D et al. Head and Neck Cancers, Version 2.2020, NCCN Clinical Practice Guidelines in Oncology. *J Natl Compr Canc Netw* 2020; 18(7): 873-98.
4. Castaldi P, Leccisotti L, Bussu F et al. Role of ^{18}F-FDG PET-CT in head and neck squamous cell carcinoma. *Acta Otorhinolaryngol Ital* 2013; 33(1): 1-8.
5. Ng SH, Chan SC, Yen TC et al. Staging of untreated nasopharyngeal carcinoma with PET/CT: comparison with conventional imaging work-up. *Eur J Nucl Med Mol Imaging* 2009; 36(1): 12-22.
6. Chan SC, Yeh CH, Yen TC et al. Clinical utility of simultaneous whole-body ^{18}F-FDG PET/MRI as a single-step imaging modality in the staging of primary nasopharyngeal carcinoma. *Eur J Nucl Med Mol Imaging* 2018; 45(8): 1297-308.
7. Cao C, Xu Y, Huang S et al. Locoregional Extension Patterns of Nasopharyngeal Carcinoma Detected by ^{18}F-FDG PET/MR. *Front Oncol* 2021; 11: 763114.
8. Cheng Y, Bai L, Shang J et al. Preliminary clinical results for PET/MR compared with PET/CT in patients with nasopharyngeal carcinoma. *Oncol Rep* 2020; 43(1): 177-87.
9. Piao Y, Cao C, Xu Y et al. Detection and staging of recurrent or metastatic nasopharyngeal carcinoma in the era of ^{18}F-FDG PET/MR. *Eur Arch Otorhinolaryngol* 2022; 279(1): 353-9.
10. Liu G, Cao T, Hu L et al. Validation of MR-Based Attenuation Correction of a Newly Released Whole-Body Simultaneous PET/MR System. *Biomed Res Int* 2019; 2019: 8213215.
11. Chen S, Hu P, Gu Y et al. Impact of patient comfort on diagnostic image quality during PET/MR exam: A quantitative survey study for clinical workflow management. *J Appl Clin Med Phys* 2019; 20(7): 184-92.
12. King AD, Ma BB, Yau YY et al. The impact of ^{18}F-FDG PET/CT on assessment of nasopharyngeal carcinoma at diagnosis. *Br J Radiol* 2008; 81(964): 291-8.
13. Lin L, Lu Y, Wang XJ et al. Delineation of Neck Clinical Target Volume Specific to Nasopharyngeal Carcinoma Based on Lymph Node Distribution and the International Consensus Guidelines. *Int J Radiat Oncol Biol Phys* 2018; 100(4): 891-902.
14. Abdel Khalek Abdel Razek A, King A. MRI and CT of nasopharyngeal carcinoma. *Am J Roentgenol* 2012; 198(1): 11-8.
15. Rodrigues RS, Bozza FA, Christian PE et al. Comparison of whole-body PET/CT, dedicated high-resolution head and neck PET/CT, and contrast-enhanced CT in preoperative staging of clinically M0 squamous cell carcinoma of the head and neck. *J Nucl Med* 2009; 50(8): 1205-13.

16. Vellayappan BA, Soon YY, Earnest A et al. Accuracy of ^{18}F-flurodeoxyglucose-positron emission tomography/computed tomography in the staging of newly diagnosed nasopharyngeal carcinoma: a systematic review and meta-analysis. *Radiol Oncol* 2014; 48(4): 331-8.
17. Chua ML, Ong SC, Wee JT et al. Comparison of 4 modalities for distant metastasis staging in endemic nasopharyngeal carcinoma. *Head Neck* 2009; 31(3): 346-54.
18. Chang MC, Chen JH, Liang JA, Yang KT, Cheng KY, Kao CH. Accuracy of whole-body ^{18}F-FDG-PET and ^{18}F-FDG-PET/CT in M staging of nasopharyngeal carcinoma: a systematic review and meta-analysis. *Eur J Radiol* 2013; 82(2): 366-73.
19. Chua MLK, Wee JTS, Hui EP, Chan ATC. Nasopharyngeal carcinoma. *Lancet* 2016; 387(10022): 1012-24.
20. Beiderwellen K, Huebner M, Heusch P et al. Whole-body ^{18}F-FDG PET/MRI vs. PET/CT in the assessment of bone lesions in oncological patients: initial results. *Eur Radiol* 2014; 24(8): 2023-30.
21. Lofgren J, Mortensen J, Rasmussen SH et al. A Prospective Study Comparing ^{99m}Tc-Hydroxyethylene-Diphosphonate Planar Bone Scintigraphy and Whole-Body SPECT/CT with ^{18}F-Fluoride PET/CT and ^{18}F-Fluoride PET/MRI for Diagnosing Bone Metastases. *J Nucl Med* 2017; 58 (11): 1778-85.
22. Li WF, Sun Y, Chen M et al. Locoregional extension patterns of nasopharyngeal carcinoma and suggestions for clinical target volume delineation. *Chin J Cancer* 2012; 31(12): 579-87.
23. Tang LL, Chen YP, Chen CB et al. The Chinese Society of Clinical Onco-logy (CSCO) clinical guidelines for the diagnosis and treatment of nasopharyngeal carcinoma. *Cancer Commun (Lond)* 2021; 41(11): 1195-227.
24. Li YQ, Tian YM, Tan SH et al. Prognostic Model for Stratification of Radioresistant Nasopharynx Carcinoma to Curative Salvage Radiotherapy. *J Clin Oncol* 2018; 36(9): 891-9.
25. Lee AWM, Ng WT, Chan JYW et al. Management of locally recurrent nasopharyngeal carcinoma. *Cancer Treat Rev* 2019; 79: 101890.
26. Abgral R, Querellou S, Potard G et al. Does ^{18}F-FDG PET/CT improve the detection of posttreatment recurrence of head and neck squamous cell carcinoma in patients negative for disease on clinical follow-up? *J Nucl Med* 2009; 50(1): 24-9.
27. Queiroz MA, Hullner M, Kuhn F et al. PET/MRI and PET/CT in follow-up of head and neck cancer patients. *Eur J Nucl Med Mol Imaging* 2014; 41(6): 1066-75.
28. Murtojarvi S, Malaspina S, Kinnunen I et al. Diagnostic Accuracy of ^{18}F-FDG PET/CT and ^{18}F-FDG PET/MRI in Detecting Locoregional Recurrence of HNSCC 12 Weeks after the End of Chemoradiotherapy: Single-Center Experience with PET/MRI. *Contrast Media Mol Imaging* 2022; 2022: 8676787.
29. Zhou N, Meng X, Zhang Y et al. Diagnostic Value of Delayed PET/MR in Liver Metastasis in Comparison With PET/CT. *Front Oncol* 2021; 11: 717687.
30. Flygare L, Erdogan ST, Soderkvist K. PET/MR versus PET/CT for locoregional staging of oropharyngeal squamous cell cancer. *Acta Radiol* 2023; 64(5): 1865-72.
31. Pyatigorskaya N, De Laroche R, Bera G et al. Are Gadolinium-Enhanced MR Sequences Needed in Simultaneous ^{18}F-FDG PET/MRI for Tumor Delineation in Head and Neck Cancer? *Am J Neuroradiol* 2020; 41(10): 1888-96.